
BEEFORMER: A FAST INFERENCE Binarized TRANSFORMER WITH EARLY EXITS

Wazib Ansar

A. K. Choudhury School of IT
University of Calcutta
Kolkata, West Bengal, India
waakcs_rs@caluniv.ac.in

Saptarsi Goswami

Department of Computer Science
Bangabasi Morning College
Kolkata, West Bengal, India
sgakc@caluniv.ac.in

Amlan Chakrabarti

A. K. Choudhury School of IT
University of Calcutta
Kolkata, West Bengal, India
acakcs@caluniv.ac.in

ABSTRACT

Large Language Models (LLMs) based on transformers achieve cutting-edge results on a variety of applications. However, their enormous size and processing requirements hinder deployment on constrained resources. To enhance efficiency, binarization and Early Exit (EE) have proved to be effective solutions. However, binarization may lead to performance loss as reduced precision affects gradient estimation and parameter updates. Besides, research on EE mechanisms is still in its early stages. To address these challenges, we introduce Binarized Early Exit Transformer (BEEformer), the first-ever selective learning-based transformer integrating Binarization-Aware Training (BAT) with EE for efficient and fast textual inference. Each transformer block has an integrated Selective-Learn Forget Network (SLFN) to enhance contextual retention while eliminating irrelevant information. The BAT employs a differentiable second-order approximation to the sign function, enabling gradient computation that captures both the sign and magnitude of the weights. This aids in $21.30 \times$ reduction in model size. The EE mechanism hinges on fractional reduction in entropy among intermediate transformer blocks with soft-routing loss estimation. This accelerates inference by reducing FLOPs by 52.08% and even improves accuracy by 2.89% by resolving the "overthinking" problem inherent in deep networks. Extensive evaluation through comparison with the SOTA methods and various ablations across six datasets covering multiple NLP tasks demonstrates its Pareto-optimal performance-efficiency trade-off.

Keywords Early Exit (EE) · Binarized Neural Network (BNN) · Selective Learn-Forget Network (SLFN) · Textual Inference · Transformers

1 Introduction

The last decade has witnessed substantial progress in the field of Natural Language Processing (NLP). Current state-of-the-art (SOTA) comprises pre-trained Large Language Models (LLMs) involving transformers [1]. However, such models have exorbitant computational complexity, leading to high energy consumption and carbon emissions [2, 3]. This necessitates the need for sustainable practices focusing on efficient and economical use of computing resources [4]. Efficient modeling reduces memory as well as amount of computations involved, leading to faster inference. Various modeling aspects have been considered towards enhancing the efficiency of models, including pruning [5], knowledge distillation (KD) [6], low-rank approximation [7], early exit (EE) [8, 9, 10] and model quantization [11, 12, 13].

Of these, quantization has become quintessential for the deployment of NLP models with constrained resources [14]. Unlike most efficiency considerations that aim to reduce the number of layers, nodes, or parameters; quantization lowers the precision of the model's memory representation [15]. In neural networks, quantization can be segregated as Post Training Quantization (PTQ) [12, 16, 17] wherein weights and/or activations are quantized post-training and Quantization Aware Training (QAT) [13, 18] that integrates quantization during the training process itself. QAT performs quantization on the weights and/or activations during the forward pass. During backpropagation, it uses full-precision latent weights and computes pseudo gradients to deal with zero gradient problem due to quantization. The class of neural networks employing 1-bit quantization is referred to as Binarized Neural Networks (BNN) and QAT

in context to BNN is called Binarization-Aware Training (BAT) [19]. It is an extreme form of quantization with 32x lower precision compared to float32 [20]. Although BNN seems to be a promising efficiency enhancement approach, only a handful of research works have been able to effectively implement it in the field of NLP [21, 22, 23]. Most of them have attempted BNN through KD from a full-precision LLM like BERT [21, 22]. Even though KD leads to a lightweight model, the training process itself is computationally as well as memory intensive [24]. To the best of our knowledge, none of the works have attempted to devise a binarized transformer architecture from scratch.

Along with quantization, dynamic variations in the model architecture accelerate inference by optimizing computational requirements based on input [25]. However, limited efforts have been directed towards making inference faster [26]. In LLMs, an input sequence is processed through multiple transformer blocks to generate the final output. However, heterogeneity can be observed in the inputs due to varying sequence lengths and sentence complexities [8]. Some inputs might require processing through all layers. For others, features from the lower or intermediate layers might be sufficient to yield predictions beyond a certain level of confidence. In such cases, while predictions based on lower layers are correct, they might become incorrect after undergoing transformations in the higher layers due to over-complicated features. These unnecessary features lead to wasteful computation or "overthinking." Therefore, allowing EE from multiple break-points based on certain conditions provides a remedy to "overthinking" [27, 8, 9] and even enhances efficacy [10]. The previous research on EE mechanisms for NLP has been on models with weights initialized from a pre-trained LLM [27, 8, 28]. The EE criterion is often a set threshold that needs to be calibrated based on the task as well as the input distribution [27]. This leads to faltering efficacy when inputs deviate during inference. Despite the potential for improved efficiency, no prior work has combined BAT with EE in a transformer architecture for textual inference. A key challenge in integrating EE with BNN is that it tends to destabilize training, leading to vanishing gradients. Additionally, standard loss functions are unsuitable for such networks.

To mitigate these challenges, we propose BEEformer— a first-of-its-kind binarized transformer architecture with selective learning and EE pathways for textual inference. It comprises an intuitive BAT mechanism with real-valued latent weights leveraging a differentiable second-order approximation to the sign function. This ensures that the gradient is aware of the sign and magnitude of the weights. For EE, the fractional change in entropy of the logits is estimated after each transformer block during inference. If the entropy does not reduce beyond a threshold percentage, the exit condition is satisfied, and the final logits are returned. This reduces FLOPs by bypassing the execution of blocks beyond the exit point. Additionally, it mitigates performance degradation due to "overthinking". During training, soft-routing loss is applied, combining the loss from all exits to effectively update the weights and enhance the decision-making capability of each transformer block. Moreover, each transformer block has a binarized version of the Selective Learn-Forget Network (SLFN) [29] integrated in it, leading to the elimination of insignificant information and better comprehension of long-range dependencies. Furthermore, BEEformer learns its parameters from scratch. It reduces additional computation and memory requirements associated with using a full-precision LLM as a starting point. All this contribute towards Pareto-optimal performance-to-complexity trade-off compared to the SOTA on datasets like SST-2, CoLA, MRPC, RTE, MNLI-m and MNLI-mm. The principal contributions of this paper are as follows:

1. We propose BEEformer— the first-ever transformer architecture trained from scratch, combining BAT with EE for textual inference. Additionally, each transformer block has an integrated binarized SLFN to enable selective learning with the elimination of insignificant information.
2. For BAT, we propose a mechanism binarizing weights as well as activations of the transformer architecture through a tight second-order approximation to the sign function. This makes it differentiable and ensures gradient-based weight updates consider both magnitude and sign of the weights leading to $21.30 \times$ reduction in model size.
3. For EE, we propose a mechanism based on fractional entropy changes in logits across transformer blocks, eliminating the need for absolute thresholds. This is accompanied by a soft-routing loss estimation during training to enhance the inferential ability of each transformer block. It reduces FLOPs by 52.08% and even improves accuracy by 2.89% through mitigating "overthinking".

The compendium to this paper has been presented herein. Section 2 gives an overview of the related works in the domain. Section 3 describes the proposed BEEformer architecture. Section 4 contains the experiment details. Section 5 discusses the results obtained through extensive evaluation on multiple datasets. Finally, the conclusions are drawn and the future scope is envisioned in Section 6.

2 Related Works

In this section, a commentary on the related works has been presented. Since BEEformer is the first model combining BNN with EE for textual inference, the works on BNN and EE have been discussed separately.

2.1 Binarized Neural Networks (BNN)

Shen et al. [11] proposed a mixed-precision, group-wise quantization method for BERT, using second-order Hessian insights to optimize compression. By analyzing Hessian eigenvalues, they refined precision allocation, while group-wise quantization enhanced control within attention layers by treating each dense matrix as a distinct group. Zhang et al. [30] attempted ternarization of the BERT model through combined approximation and loss-aware approach. Bai et al. [21] implemented weight binarization in a BERT model. To tackle sharp loss in performance, they apply KD along with ternary-weight splitting to initialize their model. However, they experience hindrances in binarizing activations and were not able to implement a fully binarized network due to a sharp performance drop due to loss of precision. Qin et al. [22] proposed a fully binarized BERT model applying binarization subject to information entropy maximization along with direction-matching distillation inferring from similarity matrices to deal with direction mismatch. Liu et al. [13] formulated a tight approximation to the sign function and updated the weights based on a magnitude-aware gradient. Liu et al. [23] further proposed a multi-step distillation approach to gradually distill the model into lower precision before obtaining the final BNN from a full-precision BERT model. They utilize an elastic binary activation with parameters inferred while training. All of the above-mentioned works adopt KD from a full-precision model to counter performance loss. However, executing both student and teacher models simultaneously for KD can be memory-intensive. Furthermore, additional fine-tuning on downstream tasks is often required for optimal results.

2.2 Early Exit (EE)

Fan et al. [31] introduced a structured dropout technique for transformers. By selectively dropping layers, it allowed sub-networks of varying depths to be extracted from a single trained model without requiring fine-tuning. Michel et al. [32] applied structured pruning to selectively remove less impactful attention heads, leading to a more efficient model with a significant reduction in inference costs. Later, Zhou et al. [33] developed an EE mechanism with the layers of a Pre-trained Language Model (PLM) interlaced with internal classifiers to exit from the network. They determined the change in predictions of successive internal classifiers, and the exit criterion was fulfilled if no change could be observed for a given number of steps. In the same context, Xin et al. [27] calculated the entropy of predictions from the internal classifiers, and if it fell short of a predetermined threshold, the exit criterion was fulfilled. However, determining the optimal threshold value is a daunting task. Liu et al. [28] put forth a pre-trained transformer model with dynamic exits having loss calculated at each layer as the sum of Masked-Language Modeling (MLM) and Sentence-Order Prediction (SOP) losses. Mangrulkar et al. [8] proposed a modified version of the switch transformer, formulating a switch layer to assess the complexity of a sentence and optimally route it to a set of expert models varying in number of encoder layers. However, the effectiveness of routing hinges on the capability of the experts to deal with varying input patterns.

2.3 Challenges of Integrating BNN with EE

It is observed that none of the works to the best of our knowledge have integrated BNN with EE in a transformer architecture for textual inference. This can be attributed to the multiple challenges involved. Binarization trims down weight and activation precision, destabilizing gradient propagation. Introducing EE complicates this further due to multiple exit points that require careful optimization to prevent vanishing gradients. Moreover, standard loss functions cannot be applied to a network with both BNN and EE, necessitating a tailored loss that preserves accuracy by enhancing the inferential capability of each exit point. Finally, estimating the EE confidence threshold in a BNN is a challenging task.

3 Proposed Architecture

The proposed BEEformer architecture embeds an input sequence and processes it through a cascade of binarized transformer blocks with the provision to exit early after each block. Each transformer block possesses binarized multi-head attention (MHA) with parameters updated via both sign as well as magnitude-aware gradient. Additionally, a selective learn-forget network binarized in a similar manner replaces the feed-forward layer in conventional transformer architecture for precise estimation of context. For EE, an intuitive criterion monitoring the fractional reduction in entropy between consecutive transformer blocks has been devised. Once the exit condition is satisfied, the processing is routed to an auxiliary block comprising binarized feed-forward layers to obtain the final predictions. This enables a two-fold efficiency enhancement due to a binarized architecture along with a provision to reduce the amount of computation dynamically during inference by terminating before the execution of all transformer blocks. The proposed architecture has been illustrated in Figure 1, while its components have been elucidated herein-below.

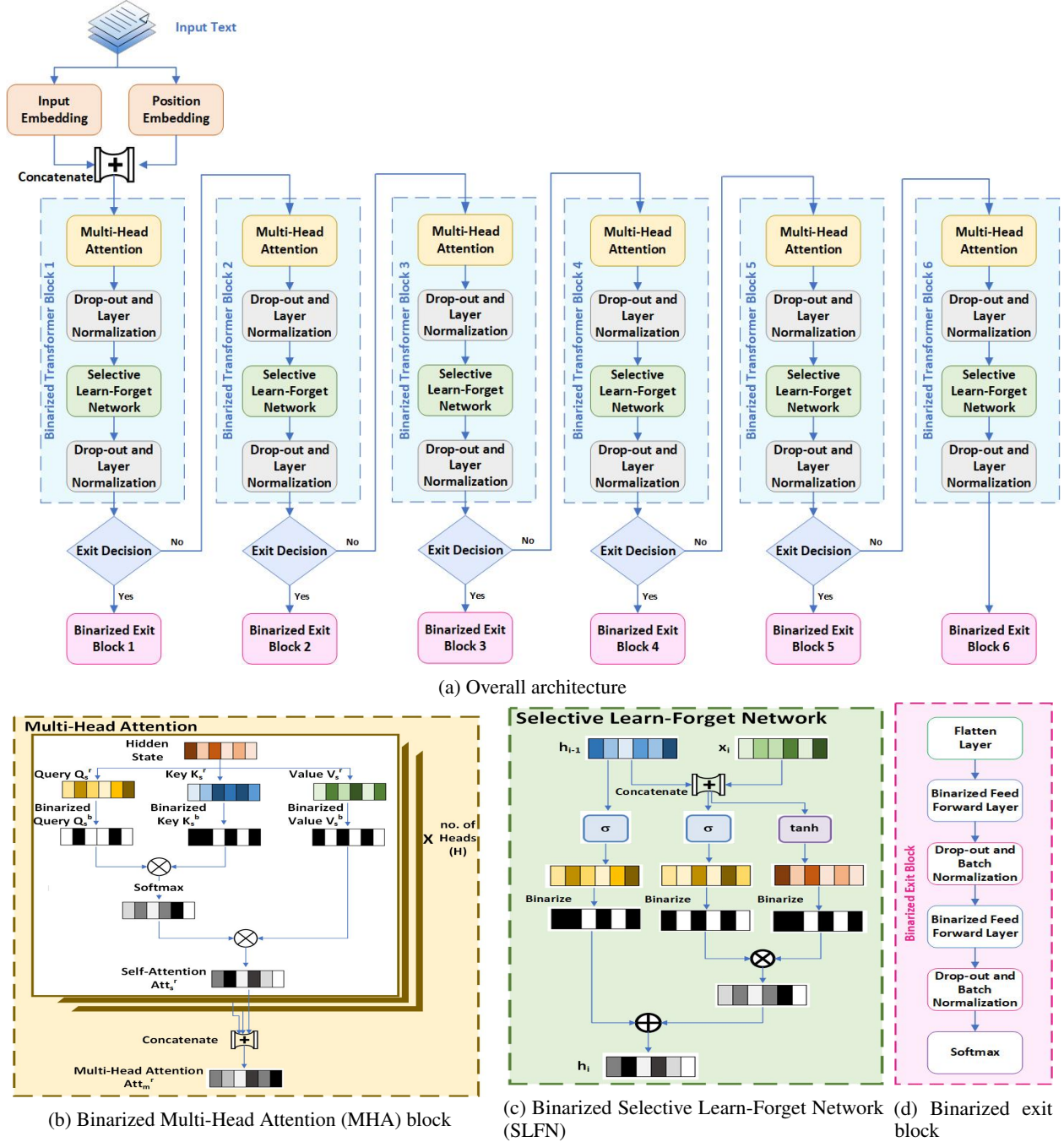


Figure 1: Illustration of the BEEformer architecture. It comprises a binarized Multi-Head Attention (MHA) block (Figure 1b), a binarized Selective Learn-Forget Network (SLFN) block to handle the representation of longer contexts in an efficient manner (Figure 1c), and a binarized auxiliary block that executes after the exit condition is satisfied (Figure 1d).

3.1 Input Representation

The input sequences in a given corpus are at first tokenized, and a lookup table $LUT()$ is constituted as a one-to-one mapping between the unique tokens V_i in the vocabulary V with a unique integer $T_i, \forall 1 \leq i \leq |V|$. For each sentence, a tokenized sequence S^t is constructed consulting the lookup table as shown in Algorithm 1. Besides, padding is appended to ensure uniform sequence length l .

Algorithm 1 Tokenized Sequence Generation

Require: Input Sequence S^{ip} , Lookup Table $LUT()$, Maximum Sequence Length l
Ensure: Tokenized Sequence S^t

```

 $sl \leftarrow \text{len}(S^{ip})$  ▷ Determining sequence length
for  $i \leftarrow 1$  to  $l$  do ▷ For tokens in  $V$ 
    if  $(i \leq sl)$  then
         $T_i \leftarrow LUT(V_i)$ 
         $S_i^t \leftarrow T_i$ 
    else ▷ For padding
         $S_i^t \leftarrow 0$ 
    end if
end for
    
```

The tokenized sequence S^t is converted into a series of embeddings $S^e \in \mathfrak{R}^{L \times D'}$, where each token S_i^t in the sequence is substituted by an embedding vector $e[i]$. The embeddings are randomly initialized and optimized throughout training, much like other network parameters. Position embedding $S^p \in \mathfrak{R}^{L \times D'}$ is used on the sequence to determine the token ordering for contextualized representation. For a given position i and dimension d , $S^p(i, d)$ is computed as shown in equation (1).

$$S^p(i, d) = \begin{cases} \sin\left(\frac{i}{10000^{d/D'}}\right) & , \text{if } d \pmod{2} = 0 \\ \cos\left(\frac{i}{10000^{(d-1)/D'}}\right) & , \text{if } d \pmod{2} = 1 \end{cases} \quad (1)$$

Finally, the token embedding sequence S^e and the position-encoded sequence S^p are element-wise concatenated (denoted by \parallel) to obtain the embedded sequence $S \in \mathfrak{R}^{L \times D}$ such that $D = 2D'$ as shown in equation (3).

$$S = S^e \parallel S^p \quad (2)$$

3.2 Backbone Network

The backbone network consists of C transformer blocks with an exit provision after each block, as depicted in Figure 1a. It can be functionally represented as $F(x)$ having a cascade of C functions (each f refers to a transformer block presented in Section 3.4) applied on the embedded input x as follows:

$$F(x) = (f_C \circ f_{C-1} \circ \dots \circ f_2 \circ f_1)(x) \quad (3)$$

Where, \circ denotes composition operator. The hidden representation h_c of the c^{th} intermediate block is given as:

$$h_c = (f_c \circ f_{c-1} \circ \dots \circ f_2 \circ f_1)(x), \forall 1 \leq c \leq C \quad (4)$$

Alternatively, h_c can be computed from the hidden representation h_{c-1} of the $(c-1)^{th}$ block as:

$$\Rightarrow h_c = f_c(h_{c-1}) \quad (5)$$

To accomplish the objective of EE, a criterion is defined. In case the criterion is fulfilled at exit c , h_c is fed to its connected auxiliary block $\Phi_c(\cdot)$ and the probability distribution \hat{y}_c is returned. This has been explained in Section 3.5.

Additionally, the BEEformer utilizes BAT (described in Section 3.3) to binarize the weights and activations of all the transformer blocks as well as the auxiliary blocks for EE. Generically, a binarized layer l is defined as follows:

$$A_l^r = a(f(b(W_l^r), b(A_{l-1}^r)) + \beta_l) \quad (6)$$

Where, A_l^r , $a(\cdot)$, $f(\cdot)$, $b(\cdot)$, W_l^r , A^r and β_l denote the computed activation, activation function, layer operator, binarization function, real-valued weights, incoming activation, and bias, respectively.

3.3 Binarization-Aware Training (BAT)

Conventionally for binarization, $sign(r)$ (Equation (7)) is applied, where r represents a real-valued weight or activation. However, being not differentiable, it cannot be applied to compute the gradient. To ameliorate this, we apply magnitude-aware approximation to $sign(r)$ [13] for the first time to the best of our knowledge in a transformer encoder. Denoted by $b(r)$, it has been expressed in Equation (8). Given $b(r)$, its derivative is computed as in Equation (9). $b(r)$ closely approximates $sign(r)$ equipped with the capability of being differentiable. This has been further analyzed in Section 5.6 through comparative plots of $b(r)$ and its derivatives alongside other binarization functions (Figure 5).

$$sign(r) = \begin{cases} -1, & \text{if } r < 0 \\ 1, & \text{if } r \geq 0 \end{cases} \quad (7)$$

$$b(r) = \begin{cases} -1, & \text{if } r < -1 \\ 2r + r^2, & \text{if } -1 \leq r < 0 \\ 2r - r^2, & \text{if } 0 \leq r < 1 \\ 1, & \text{if } r \geq 1 \end{cases} \quad (8)$$

$$b'(r) = \frac{\partial b(r)}{\partial r} = \begin{cases} 2(1 - |r|), & \text{if } -1 \leq r < 1 \\ 0, & \text{if } r < -1 \text{ or } r \geq 1 \end{cases} \quad (9)$$

where $b(r)$ is a differentiable piecewise polynomial function being a second-order approximation to the sign function $sign(r)$. While $\frac{\partial b(r)}{\partial r}$ is a piecewise linear function approximating the derivative of $sign(r)$, which is an impulse function during gradient calculation.

Conventional gradient descent cannot be applied to BNN due to the gradient of loss \mathcal{L} concerning binarized weights being insufficient to enable bit-flips. To mitigate this issue, we perform BAT wherein the gradient computed for the l^{th} layer concerning binarized weights $W_{l,t}^b$ for the t^{th} iteration is used to update real-valued weights $W_{l,t+1}^r$ for the $(t+1)^{th}$ iteration. This has been shown in the following equation:

$$W_{l,t+1}^r = W_{l,t}^r - \eta \frac{\partial \mathcal{L}}{\partial W_{l,t}^r} \quad (10)$$

Applying the chain rule for partial derivatives on $\frac{\partial \mathcal{L}}{\partial W_{l,t}^r}$,

$$\Rightarrow W_{l,t+1}^r = W_{l,t}^r - \eta \frac{\partial \mathcal{L}}{\partial W_{l,t}^b} \frac{\partial W_{l,t}^b}{\partial W_{l,t}^r} \quad (11)$$

$$\Rightarrow W_{l,t+1}^r = W_{l,t}^r - \eta \frac{\partial \mathcal{L}}{\partial W_{l,t}^b} \frac{\partial b(W_{l,t}^r)}{\partial W_{l,t}^r} \quad (12)$$

where, $W_{l,t}^b = b(W_{l,t}^r)$, and η denotes the learning rate. Applying the chain rule, $\frac{\partial \mathcal{L}}{\partial W_{l,t}^b}$ is expanded as follows:

$$\frac{\partial \mathcal{L}}{\partial W_{l,t}^b} = \frac{\partial \mathcal{L}}{\partial A_{l,t}^r} \frac{\partial A_{l,t}^r}{\partial Z_{l,t}^r} \frac{\partial Z_{l,t}^r}{\partial W_{l,t}^b} \quad (13)$$

where, $A_{l,t}^r$ represents the real-valued activation computed for the l^{th} layer and t^{th} iteration, and $Z_{l,t}^r$ represents the output of the layer operator $f(\cdot)$ in Equation (6). Since $A_{l,t}^r = a(Z_{l,t}^r)$, it can be written as:

$$\Rightarrow \frac{\partial \mathcal{L}}{\partial W_{l,t}^b} = \frac{\partial \mathcal{L}}{\partial A_{l,t}^r} a'(Z_{l,t}^r) b(A_{l-1,t}^r) \quad (14)$$

Expanding $\frac{\partial \mathcal{L}}{\partial A_{l,t}^r}$, in Equation (14) applying the chain rule as follows:

$$\Rightarrow \frac{\partial \mathcal{L}}{\partial W_{l,t}^b} = \frac{\partial \mathcal{L}}{\partial A_{l,t}^b} \frac{\partial A_{l,t}^b}{\partial A_{l,t}^r} a'(Z_{l,t}^r) b(A_{l-1,t}^r) \quad (15)$$

where, $A_{l,t}^b$, i.e. the binarized activation for the l^{th} layer and t^{th} iteration is computed as $b(A_{l,t}^r)$. Therefore, Equation (15) can be simplified as:

$$\Rightarrow \frac{\partial \mathcal{L}}{\partial W_{l,t}^b} = \frac{\partial \mathcal{L}}{\partial A_{l,t}^b} \frac{\partial b(A_{l,t}^r)}{\partial A_{l,t}^r} a'(Z_{l,t}^r) b(A_{l-1,t}^r) \quad (16)$$

Substituting $\frac{\partial \mathcal{L}}{\partial W_{l,t}^b}$ from Equation (16) in Equation (12), as follows:

$$W_{l,t+1}^r = W_{l,t}^r - \eta \left[\frac{\partial \mathcal{L}}{\partial A_{l,t}^b} \frac{\partial b(A_{l,t}^r)}{\partial A_{l,t}^r} a'(Z_{l,t}^r) b(A_{l-1,t}^r) \right] \frac{\partial b(W_{l,t}^r)}{\partial W_{l,t}^r} \quad (17)$$

Based on Equation (9), Equation (17) can be formulated as follows:

$$\Rightarrow W_{l,t+1}^r = W_{l,t}^r - \eta \left[\frac{\partial \mathcal{L}}{\partial A_{l,t}^b} g'(A_{l,t}^r) a'(Z_{l,t}^r) b(A_{l-1,t}^r) \right] b'(W_{l,t}^r) \quad (18)$$

Once BAT is completed, the updated binarized weights $W_{l,t+1}^b$ are frozen applying Equation (7) to ensure $W_{l,t+1}^b \in \{-1, 1\}$ as shown in Equation (19). The details of the implementation of the above-mentioned binarization technique in the BEExformer transformer blocks are presented in Section 3.4.

$$W_{l,t+1}^b = \text{sign}(W_{l,t}^r) \quad (19)$$

3.4 Transformer Blocks

Each transformer block binarizes the multi-head attention (MHA) [34] Att_m^b module as depicted in Figure 1b. Att_m^b is comprised of H binarized self-attention Att_s^b heads, which in turn relies on queries Q_s^b , keys K_s^b , and values V_s^b for computation as follows:

$$Att_s^r = \text{softmax} \left(\frac{Q_s^b (K_s^b)^T}{\sqrt{D}} \right) V_s^b \quad (20)$$

where Q_s^b , K_s^b , and V_s^b have been obtained through binarized-linear (bi-linear) transformation (explained in Section 3.3) on input $x \in \mathbb{R}^{L \times D}$ where L denotes the sequence length and D denotes the dimension of hidden representations. The computations have been shown in equations (21 -23).

$$Q_s^b = b(W_q^r) b(x^r) \quad (21)$$

$$K_s^b = b(W_k^r) b(x^r) \quad (22)$$

$$V_s^b = b(W_v^r) b(x^r) \quad (23)$$

where $W_q^r, W_k^r, W_v^r \in \mathbb{R}^{D \times D/H}$. Finally, Att_m^b is calculated in Equation (24) through projection of H concatenated Att_s^r through $W_o^r \in \mathbb{R}^{D \times D}$ after binarization.

$$Att_m^b = b(\text{Concatenate}(Att_{s,i}^r)) b(W_o^r), \forall i \in H \quad (24)$$

To augment the efficacy of residual connection, a binarized SLFN is used to replace the feed-forward layer in the conventional transformer architecture. This is the modified version of SLFN proposed by Ansar et al. [29]. In SLFN, there are two forget gates, Sh_i^b and Sg_i^b , which aid in the elimination of insignificant information in the previous hidden state and the total incoming activations, respectively. Besides, it has a selective learning gate Tg_i^b for rational estimation of dependencies. All the gates incorporate binarization of incoming activations as shown in Equation (8). The architecture has been illustrated in Figure 1c, while the formulation of the gates has been provided in the following equations.

$$Sh_i^b = \sigma[b(h_{i-1}^r)b(U_{sg}^r)] \quad (25)$$

$$Sg_i^b = \sigma[(b(x_i^r)b(W_{sg}^r) + (b(h_{i-1}^r)b(U_{sg}^r))] \quad (26)$$

$$Tg_i^b = \tanh[(b(x_i^r)b(W_{tg}^r) + (b(h_{i-1}^r)b(U_{tg}^r))] \quad (27)$$

where x_i^r and h_{i-1}^r denote full-precision input at i^{th} step and $(i-1)^{th}$ hidden state, respectively. Whereas W_{sg}^r , U_{sg}^r , W_{tg}^r , and U_{tg}^r denote weight matrices for inputs as well as hidden states, respectively. Here, we apply $b(\cdot)$ on all incoming weights and activations for binarization. Finally, the updated hidden state is calculated as follows:

$$h_i = b(Sg_i^b) + [b(Sg_i^b) \odot b(Tg_i^b)] \quad (28)$$

3.5 Early Exit

We propose an EE criterion that estimates proportionate entropy reduction over exits, i.e. fractional reduction in entropy concerning the previous exit. When this value falls below a certain threshold δ , the exit criterion is satisfied. This has been portrayed in Algorithm 2. Here, the entropy of logits $S(h_c)$ is computed as in Equations (29) and (30). Initially, the value of $S(h_c)$ is taken as $\ln(m)$, which signifies the case when logits are spread as evenly as possible across m classes.

$$S(h_c) = - \sum_{j=1}^m p(h_c^j) \ln(p(h_c^j)) \quad (29)$$

$$\Rightarrow S_t(h_c) = \ln\left(\sum_{j=1}^m \exp(h_c^j)\right) - \frac{\sum_{j=1}^m h_c^j \cdot \exp(h_c^j)}{\sum_{j=1}^m \exp(h_c^j)} \quad (30)$$

Algorithm 2 Early Exit Estimation

Require: Input Sequence x , Number of classes m , EE threshold δ

Ensure: Output at c^{th} exit \hat{y}_c

$h_0 \leftarrow x$	▷ Initialize incoming activation
$S(h_0) \leftarrow \ln(m)$	▷ Initialize entropy value
for $c \leftarrow 1$ to C do	
$h_c \leftarrow f_c(h_{c-1})$	▷ Logits returned by c^{th} block
Calculate $S(h_c)$	
if $\frac{S(h_{c-1}) - S(h_c)}{S(h_{c-1})} < \delta$ then	▷ Exit condition
$\hat{y}_c = \Phi_c(h_c)$	▷ Auxiliary block execution
return \hat{y}_c	
end if	
end for	

Following this, an auxiliary block $\Phi_c(\cdot)$ is defined to process h_c and predict the output \hat{y}_c as follows:

$$\hat{y}_c = \Phi_c(h_c), \quad \exists \Phi_c \in \Phi \quad (31)$$

Here, $\Phi_c(\cdot)$ belongs to the set of binarized feed-forward networks $\Phi = \{\Phi_1, \Phi_2, \dots, \Phi_C\}$ as shown in Figure 1d. It processes h_c into a discrete probability distribution \hat{y}_c as the output for the c^{th} exit. To ensure minimal computational overhead, $\Phi_c(\cdot)$ has a minimal number of parameters compared to the backbone network $F(\cdot)$.

The proposed EE criterion is robust against diversity in inputs during inference as only the fractional reduction in entropy is noted. This alleviates the limitation of previous works with absolute entropy thresholds to deal with diverse inputs. Also, determining the absolute threshold is a cumbersome process in such models. Compared to it, setting δ is pretty straightforward based on the computational budget and output confidence requirements. Moreover, the same value of δ can be used across multiple datasets.

3.6 Soft-Routing Loss Function

The loss function L calculated at the i^{th} exit is given by the following equation:

$$\mathcal{L}_i(\mathcal{I}; \theta) = \frac{1}{|\mathcal{I}|} \sum_{(x,y) \in \mathcal{I}} \mathcal{H}(y, F_i(x; \theta)) \quad (32)$$

Where \mathcal{I} is the input data containing sequence-label pairs, (x, y) , $F_i(x; \theta)$ is the probability distribution returned by the i^{th} exit, θ denotes trainable parameters, and \mathcal{H} is the cross-entropy function. The proposed model uses a soft-routing loss objective, i.e. combining loss from all exits to enhance the decision capability. This aids in optimal assessment of the exit based on the predictions from all the exit blocks while reducing the loss. The total loss \mathcal{L}' is calculated as the mean loss across all exits given by:

$$\mathcal{L}'(\mathcal{I}; \theta) = \frac{1}{|C|} \sum_i^C \mathcal{L}_i(\mathcal{I}; \theta) \quad (33)$$

where C is the total no. of exits.

4 Experimental Setup

In this section the details of the experiment conducted along with the dataset information have been provided.

4.1 Datasets

The proposed methodology has been applied to multiple benchmark datasets, including the Stanford Sentiment Treebank (SST-2) [35], the Corpus of Linguistic Acceptability (CoLA) [36], the Microsoft Research Paraphrase Corpus (MRPC) [37], the Recognizing Textual Entailment (RTE) dataset [38], and the Multi-Genre Natural Language Inference (MNLI) dataset [39]. The MNLI dataset includes both matched (m) and mismatched (mm) variants, where "m" denotes samples from the same genres as the training data, while "mm" refers to samples from different genres, assessing the model's generalization capabilities. These datasets cover a wide range of tasks such as sentiment analysis, linguistic acceptability, semantic similarity between texts, paraphrase detection, and entailment detection. The metrics for evaluation are F1 score for MRPC, Matthews correlation for CoLA, and accuracy for the remaining datasets.

4.2 Implementation Details

The proposed BEEformer has been implemented on a Python 3 Compute Engine with the Nvidia L4 GPU, 22.5GB VRAM, 53GB System RAM, and 201.2GB Disk in Google Colab¹. The details of the hyperparameters of the BEEformer have been presented in Table 1.

5 Results and Discussion

5.1 Comparison with Related Works

To the best of our knowledge, combining binarization with EE is unprecedented for textual content. Thus, we compare with works which either implement QNN or EE in separate tables for ease of comprehension. Additionally, we provide

¹<https://colab.research.google.com>

Table 1: Hyperparameter Details of the BEEformer Model

Hyperparameter	Value
# Transformer Blocks	6
# Attention Heads	4
Embedding Dimension	512
Hidden Layer Dimension	768
EE Threshold (δ)	0.0001
Dropout Ratio	0.3
Optimizer	Adam
Loss Function	Binary Cross-Entropy
Learning Rate	[0.01 - 0.0001] (decreases on plateau)
Early Stopping Patience Value	5
Batch Size	32
Training Epochs	50

Table 2: Comparison with Quantized Models without EE

Model	#Bits ↓ (W-A)	Size ↓ (MB)	GFLOPs ↓	SST-2 ↑	CoLA ↑	MRPC ↑	RTE ↑	MNLI-m ↑	MNLI-mm ↑
Quantized Models without EE									
Q-BERT [11]	8-8	43	6.5	84.6	-	68.3	52.7	76.6	77.0
TernaryBERT [30]	2-8	28	6.4	-	50.7	87.5	68.2	83.3	83.3
TernaryBERT [30]	2-2	28	1.5	80.7	-	68.3	54.5	40.3	40.0
TernaryBERT [30]	2-1	28	0.8	53.1	-	68.3	53.4	32.7	33.0
BinaryBERT [21]	1-8	16.5	3.1	92.6	53.4	85.5	72.2	84.2	84.7
BinaryBERT [21]	1-4	16.5	1.5	92.3	44.4	83.3	65.3	83.9	84.2
BinaryBERT [21]	1-2	16.5	0.8	82.5	14.6	68.3	52.7	62.7	63.9
BinaryBERT [21]	1-1	16.5	0.4	53.2	0	68.3	52.7	35.6	35.3
BiBERT [22]	1-1	13.4	0.4	88.7	25.4	72.5	57.4	66.1	67.5
BiT (WMS) [23]	1-4	13.4	1.5	91.5	42.0	86.8	66.4	83.6	84.4
BiT (WMS) [23]	1-2	13.4	0.8	90.8	32.1	78.4	58.1	82.1	82.5
BiT (WMS) [23]	1-1	13.4	0.4	87.7	25.1	79.7	58.8	77.1	77.5
BiT [23]	1-1	13.4	0.4	89.9	32.9	79.9	62.1	79.5	79.4
Binarization with EE									
BEEformer (Proposed)	1-1	14.26	0.12	92.32	60.30	86.47	71.11	83.71	84.29

Note- WMS: Without multi-distillation, '-' indicates value is not available.

The default metrics for each dataset have been used for the results.

↑ indicates higher value is desired while ↓ indicates lower value is desired.

The bold values indicate the best results across each category.

a comparison with standard full-precision models with an equal number of transformer blocks to analyze the impact of BAT, EE, and SLFN on model performance and efficiency.

5.1.1 Purely Quantized Models

Table 2 presents the comparison with SOTA Quantized Models without EE on the basis of model quantization configuration, size, GFLOPs, and performance metrics for various datasets. BEEformer stands out with a remarkably low 0.12 GFLOPs, compared to quantized models without EE, demonstrating the efficiency of EE in reducing computation during inference. By dynamically eliminating processing through a certain number of layers, it avoids full deep-network computation while maintaining a compact 14.26 MB model size, comparable to BiBERT and BiT, and even smaller than BinaryBERT—indicating minimal overhead from EE and SLFN. Despite not distilling knowledge from full-precision models like BERT, BEEformer achieves strong benchmark performance, outperforming other BNNs with (1-1) quantization configuration. While binarized models (BinaryBERT, BiBERT, BiT) offer small size and low GFLOPs, their performance drops notably on CoLA and RTE, implying that binarization alone is insufficient without mechanisms like EE or SLFN. Conversely, TernaryBERT and Q-BERT achieve competitive performance but at the cost of larger size and higher GFLOPs, demonstrating a suboptimal trade-off between performance and efficiency.

Table 3: Comparison with Full-precision EE Models

Model	#Bits ↓ (W-A)	Size ↓ (MB)	GFLOPs ↓	SST-2 ↑	CoLA ↑	MRPC ↑	RTE ↑	MNLI- m ↑	MNLI- mm ↑
Full-precision EE Models									
LayerDrop _{Base} [31]	32-32	477.5	6.7	93.7	64.5	91.6	71.1	86.4	86.5
LayerDrop _{Base-6L} [31]	32-32	313.2	3.4	91.3	53.7	87.6	64.3	83.8	83.8
LayerDrop _{Large} [31]	32-32	1356.1	23.8	95.5	66.6	91.2	86.6	89.7	89.6
LayerDrop _{Large-6L} [31]	32-32	492.8	6.0	91.4	44.3	79.8	53.1	81.4	81.0
HeadPrune-BERT _{Base} [32]	32-32	332.3	4.7	89.4	48.7	80.2	62.5	71.0	79.7
ElasticBERT _{Base} [28]	32-32	416.4	6.6	94.3	64.3	91.0	76.5	85.3	85.9
ElasticBERT _{Base-6L} [28]	32-32	255.9	3.3	92.7	53.7	89.7	74.0	84.3	84.2
ElasticBERT _{Large} [28]	32-32	1279.7	23.4	95.3	66.3	92.0	83.1	88	88.5
ElasticBERT _{Large-6L} [28]	32-32	412.6	5.9	91.9	53.9	89.6	71.1	83.5	84.3
BE3R_BERT [8]	32-32	1297	-	93.23	59.81	90.27	71.48	85.63	85.86
BE3R_Electra [8]	32-32	1278	-	96.79	68.26	91.47	86.28	89.56	89.29
PABEE [33]	32-32	46	4.4	93.0	61.2	90.0	80.1	85.1	85.1
Binarization with EE									
BEEformer (Proposed)	1-1	14.26	0.12	92.32	60.30	86.47	71.11	83.71	84.29

Note- '-' indicates value is not available.

The default metrics for each dataset have been used for the results.

↑ indicates higher value is desired while ↓ indicates lower value is desired.

The bold values indicate the best results across each category.

However, BEEformer provides an optimal balance due to integration with SLFN and EE, providing high performance with superior efficiency.

Table 4: Comparison with Full-precision Standard Transformer Models

Model	#Bits ↓ (W-A)	Size ↓ (MB)	GFLOPs ↓	SST-2 ↑	CoLA ↑	MRPC ↑	RTE ↑	MNLI- m ↑	MNLI- mm ↑
Full-precision Standard Transformer Models Having Default Architecture									
BERT _{Base-12L} [40]	32-32	418	6.62	92.9	56.5	87.6	69.0	84.6	84.9
ALBERT _{Base-12L} [41]	32-32	46	6.86	92.8	56.8	90.5	78.3	84.9	85.6
RoBERTa _{Base-12L} [42]	32-32	479	6.73	94.8	63.6	90.8	77.5	87.5	87.2
BERT _{Large-24L} [40]	32-32	1285	23.45	93.5	61.6	90.1	72.9	86.2	86.0
ALBERT _{Large-24L} [41]	32-32	69	24.30	95.2	60.1	90.4	83.0	86.0	86.1
RoBERTa _{Large-24L} [42]	32-32	1362	23.84	95.4	66.4	91.6	86.6	89.0	89.6
Full-precision Standard Transformer Models Having 6-Layers									
BERT _{Base-6L} [40]	32-32	257	3.31	90.9	44.6	84.9	65.7	81.4	81.4
ALBERT _{Base-6L} [41]	32-32	46	3.44	90.8	52.4	89.0	70.4	82.6	82.2
RoBERTa _{Base-6L} [42]	32-32	314	3.36	92.1	44.4	87.9	60.6	84.2	84.6
BERT _{Large-6L} [40]	32-32	414	5.86	89.7	20.2	76.4	58.5	76.5	76.5
ALBERT _{Large-6L} [41]	32-32	69	6.08	92.2	51.7	86.5	66.4	82.2	82.9
RoBERTa _{Large-6L} [42]	32-32	495	5.96	90.1	43.3	80.0	54.9	80.4	80.9
Proposed Model									
BEEformer-6L (Proposed)	1-1	14.26	0.12	92.32	60.30	86.47	71.11	83.71	84.29

Note- The suffix '-λL' has been appended to model names, where λ represents the number of layers (transformer blocks).

The results of the model variants are from Liu et al. [28].

The default metrics for each dataset have been used for the results.

↑ indicates higher value is desired while ↓ indicates lower value is desired.

The bold values indicate the best results across each category.

5.1.2 Purely EE Models

In Table 3 comparing purely EE models, BEEformer stands out for its efficiency, having 14.26 MB size, i.e. $46 \times$ smaller than the average of listed models, and requiring just 0.12 GFLOPs for inference. In contrast, the full-precision models span hundreds to over a thousand MB, demanding 3.31–24.30 GFLOPs. Although it excels in efficiency, it exhibits slightly less performance compared to the SOTA full-precision models like LayerDropLarge and BE3R_Electra. However, BEEformer remains highly competitive, achieving comparable performance to most of the compared models and even outperforming some like HeadPrune-BERT_{Base} on various datasets. Therefore, BEEformer excels in balancing efficiency and performance, delivering high competitiveness with full-precision EE models.

Table 5: Comparison of Model Ablations

Model	#Bits ↓ (W-A)	Size ↓ (MB)	SST-2 ↑	CoLA ↑	MRPC ↑	RTE ↑	MNLI- m ↑	MNLI- mm ↑
Full-Precision Ablations								
BEEformer (WSLFN-FP)	32-32	238.45	90.71	57.43	84.27	67.15	79.39	80.88
BEEformer (WEE-FP)	32-32	263.09	92.72	61.33	88.41	72.67	83.91	84.70
BEEformer (FP)	32-32	303.76	95.10	62.70	90.92	75.81	87.18	88.09
Binarized Ablations								
BEEformer (WSLFN)	1-1	10.33	85.77	53.21	82.30	64.98	76.48	77.22
BEEformer (WEE)	1-1	11.05	89.61	58.62	84.81	68.12	79.27	80.41
BEEformer (Proposed)	1-1	14.26	92.32	60.30	86.47	71.11	83.71	84.29

Note- WEE: Without the proposed EE ; WEE-FP: Full-Precision without EE ; FP: Full-Precision ; WSLFN: Without SLFN ; WSLFN-FP: Full-Precision without SLFN.
 The default metrics for each dataset have been used for the results.
 ↑ indicates higher value is desired while ↓ indicates lower value is desired.
 The bold values indicate the best results across each category.

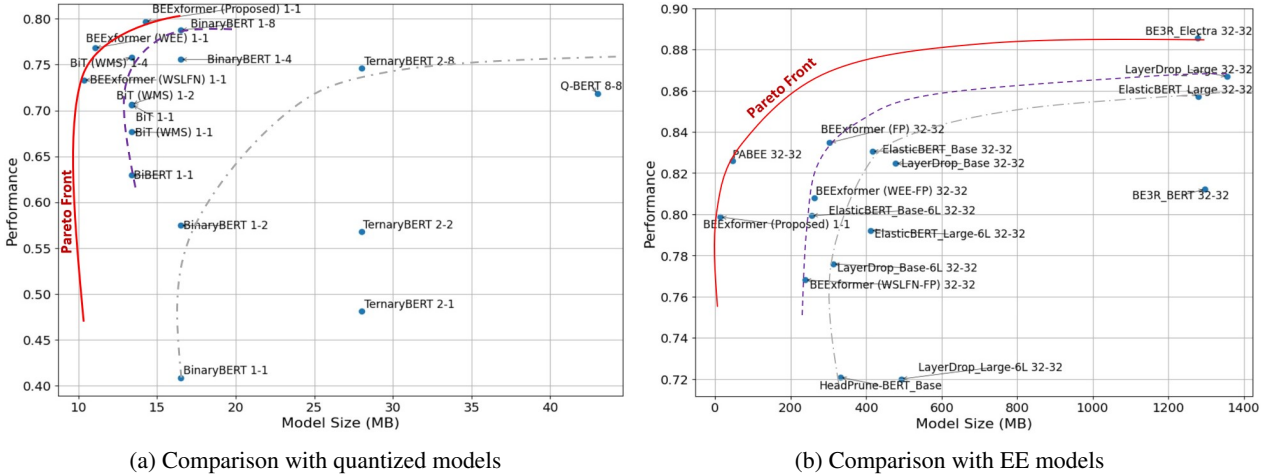


Figure 2: Pareto front charts comparing BEEformer with related works as well as its ablations. For a justified comparison, the quantized models and the EE models have been compared separately.

5.1.3 Standard Transformer Models

Table 4 compares BEEformer with full-precision standard transformers having default architectures. It also includes six-block variants of these models to evaluate performance at a similar scale as the BEEformer. The BEEformer model is $3.22 \times$ smaller in size and requires $27.58 \times$ fewer GFLOPs compared to the most optimal full-precision Transformer model listed in the table. Despite its efficiency, BEEformer achieves performance comparable to that of full-precision models with their default number of layers. Moreover, it outperforms the full-precision models configured with six blocks on SST-2, CoLA, and RTE datasets. This highlights that the combination of SLFN, BAT and EE in the proposed BEEformer makes it a computationally efficient alternative to conventional transformer models.

5.2 Study of Model Ablations

Table 5 presents the results from various ablations of the proposed BEEformer. Here, BEEformer without SLFN (WSLFN) is the most lightweight version, while the full-precision version (FP), gives the best results among the ablations. Despite being $21.30 \times$ smaller than the FP ablated version, the proposed BEEformer undergoes a modest performance drop of 3.60% across datasets. While, the proposed BEEformer delivers performance comparable to full-precision ablation without EE (WEE-FP) with a difference of 0.92% despite being $18.44 \times$ smaller in size. Moreover, BEEformer excels over the binarized ablation without EE (WEE) by 2.89%. This highlights the potency of EE to boost performance by countering "overthinking". From the SLFN ablations, it can be perceived that BEEformer leads over the full-precision ablation (WSLFN-FP), and binarized ablation (WSLFN) by 3.06% and 6.37% respectively. Thus SLFN plays a significant role in augmenting the transformer’s capability to comprehend dependencies in the input sequence. Furthermore, given the performance versus efficiency trade-off, the proposed BEEformer gives the best results compared to all its ablations as discussed in Section 5.3.

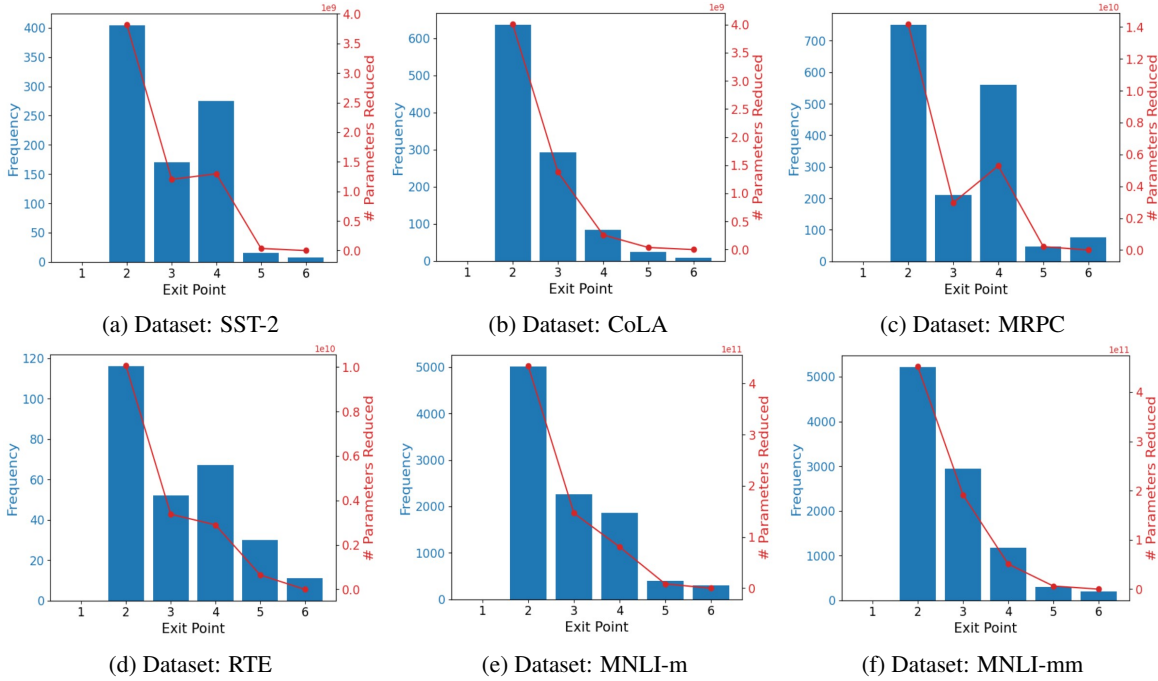


Figure 3: Distribution of exits and total number of parameters saved from computation during inference upon all datasets.

5.3 Pareto Optimality

To evaluate the multi-objective optimization of performance alongside model size, BEEformer has been compared on Pareto fronts against SOTA quantized models and EE models, as shown in Figures 2a and 2b respectively. The plots illustrate the optimal Pareto Front (solid red line), with second and third fronts marked by dashed purple and grey lines. Each point represents a model, labeled with its name and quantization configuration. Models near the optimal front achieve superior performance for a given model size or smaller sizes for a given performance level.

In Figure 2a, BEEformer (Proposed) 1-1 is positioned near the optimal Pareto Front in the top-left, attaining the highest binarized model performance (79.70%) with a compact 14.26MB size. Ablations like BEEformer (WSLFN) 1-1 and BEEformer (WEE) 1-1 remain Pareto-optimal but the performance drops by 6.37% and 2.89% for a model size reduction of 3.93% and 3.21%, respectively. Thus, removing WSLFN and EE blocks significantly lowers performance with modest size gains, highlighting BEEformer’s efficiency. Among binarized Transformers like BinaryBERT, BiBERT and BiT; BEEformer offers a superior performance-size trade-off. While quantized models like TernaryBERT and Q-BERT achieve competitive performance, they come at the expense of much larger model sizes.

In Figure 2b, BEEformer (Proposed) 1-1, positioned on the optimal Pareto front, achieves a $21.30 \times$ model size reduction compared to its full-precision counterpart (BEEformer FP) on the second front, while maintaining competitive performance (3.60% lower). This underscores the effectiveness of BAT in model efficiency. Other ablations too fall

on the second front but offer much less performance given their model sizes, highlighting the contributions of SLFN and EE. Among SOTA models, PABEE 32-32, also on the optimal front, outperforms BEEformer 1-1 by 2.72%, but at $3.22 \times$ the size, making it less efficient. Larger models like BE3R_Electra 32-32, LayerDrop Large 32-32, and ElasticBERT Large 32-32 achieve higher performance but with substantial size increases, while their base variants witness performance drop due to fewer layers.

Table 6: Percentage Reduction in FLOPs due to EE

Dataset	WEE \downarrow (GFLOPs)	EE \downarrow (GFLOPs)	Percentage Reduction \uparrow
SST-2	0.240	0.116	51.43%
MRPC	0.240	0.123	48.71%
CoLA	0.240	0.101	57.69%
RTE	0.242	0.128	47.34%
MNLI-m	0.242	0.115	52.50%
MNLI-mm	0.242	0.109	54.84%
Overall	0.241	0.116	52.08%

Note- "Overall" denotes the mean percentage reduction of FLOPs across all datasets.

EE: Applying the proposed EE; WEE: Without EE; GFLOPs: Giga FLOPs

GFLOPs have been rounded to three decimal places, whereas the percentage reduction has been calculated using all significant digits to ensure accurate measurement.

\uparrow indicates higher value is desired while \downarrow indicates lower value is desired.

5.4 Distribution of Exit Points

For a deeper insight, we plot the exit point distribution along with the number of parameters saved, i.e. not computed due to EE, during inference over all datasets in Figure 3. It appears that 49.84% of the observations exit after the second transformer block, while a mere 2.45% samples need to go through the last transformer block. This highlights savings in computation during inference compared to traditional models, which involve all layers of the network. The total number of parameters saved from computation during inference is proportional to how early the exit condition is satisfied. Its maximum effect is noticed at the second exit and then starts decreasing. For subsequent exits, the plots indicate that despite having a higher frequency in some cases, their impact on saving parameters might not be that pronounced. An interesting observation is that none of the samples exit from the first block during inference. This is due to the substantial reduction in entropy from the initialized value $\ln(m)$ after the execution through the first transformer block.

Furthermore, Table 6 presents the percentage reduction in overall FLOPs during inference over all datasets compared to the variant without EE. On average, the EE mechanism in BEEformer saves around 52.08% FLOPs during inference accompanied with 2.89% increase in performance. It affirms our motivation behind EE to utilize fewer transformer blocks than present in the architecture during inference.

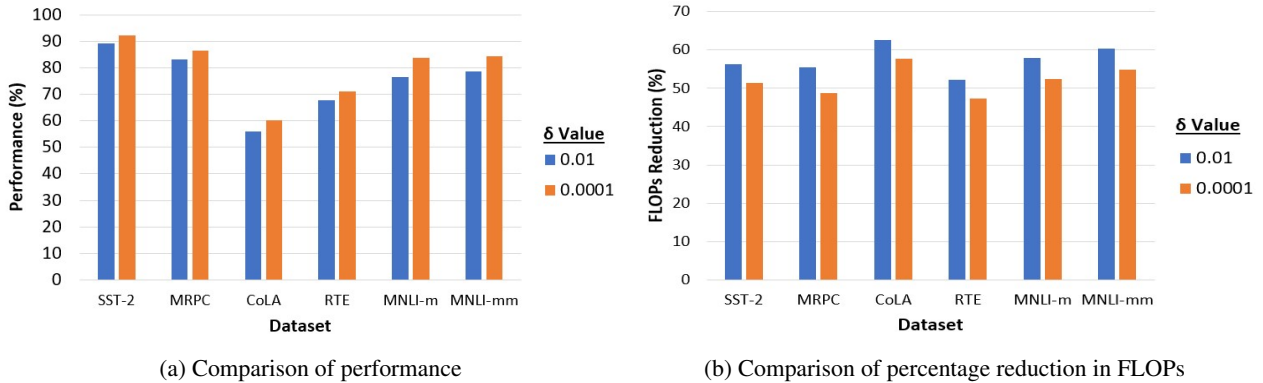


Figure 4: Comparison of the quantized models for varying δ on all the datasets. Here, $\delta = 0.0001$ corresponds to the proposed version of BEEformer.

5.5 Effect of EE Threshold

We observe that the EE threshold (δ) plays a pivotal role in determining the trade-off between efficacy of results and reduction in FLOPs during inference. Figure 4 shows comparison of performance using $\delta = 0.0001$ (proposed) with $\delta = 0.01$. Although larger δ value reduces the inference time through 5.38% average reduction in FLOPs, the confidence in results decreases, translating into a drop in performance by 4.49%. Alternatively, for smaller values of δ , the confidence in outputs increases with a slight delay in inference. Thus, setting $\delta \rightarrow 0^+$ proves to be a win-win situation leading to a rise in performance along with reduced FLOPs for inference. It tackles "overthinking" wherein the entropy of logits starts rising instead of decreasing. Therefore, letting the inputs with even a slight reduction in entropy to be processed further, otherwise execution is terminated.

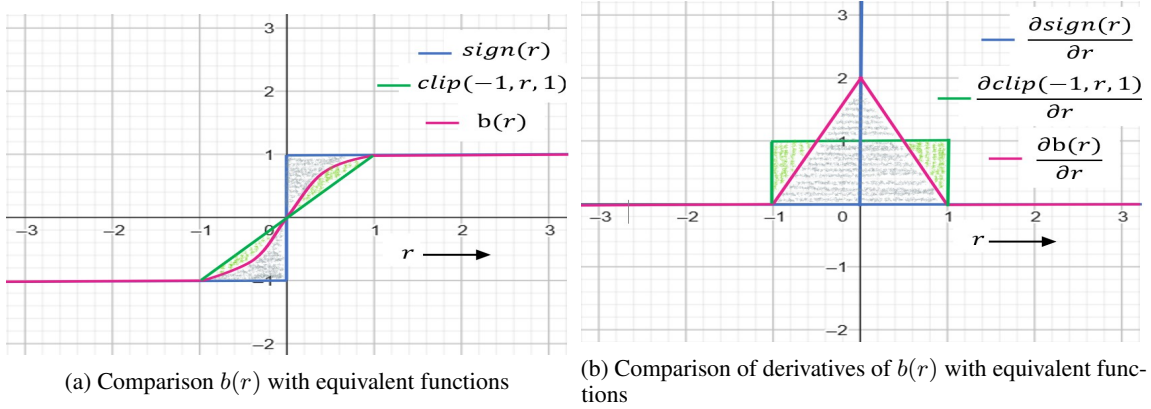


Figure 5: Comparison of plots for $sign(r)$, $clip(-1, r, 1)$, and the proposed binarization function $b(r)$ along with their derivatives. The shaded areas portray the difference between the two functions.

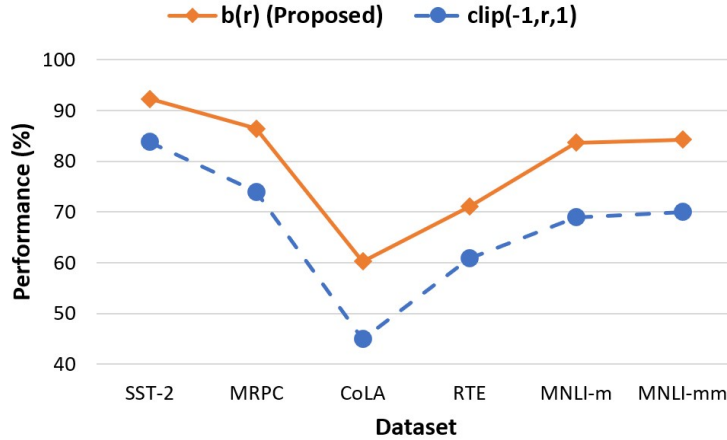


Figure 6: Comparison of performance of the proposed binarization function $b(r)$ with $clip(-1, r, 1)$ function on all the datasets.

5.6 Comparison of Binarization Functions

To assess the effectiveness of the binarization function $b(r)$ in BEEformer, it has been compared with $clip(-1, r, 1)$ [20]. To give a clear picture, Figure 5 graphically plots $sign(r)$, $clip(-1, r, 1)$ and $b(r)$ along with their derivatives with shaded areas highlighting the difference among them. While $b(r)$ improves gradient stability by providing a smoother approximation to $sign(r)$, $clip(-1, r, 1)$ lacks the smooth transition provided by $b(r)$, potentially leading to sharper gradient updates and instability in certain cases. Furthermore, $b(r)$ is a tighter approximation to $sign(r)$ compared to $clip(-1, r, 1)$, leading to more accurate gradient estimation. This gets reflected in the performance too when $b(r)$ is substituted with $clip(-1, r, 1)$ in the proposed BEEformer, where $b(r)$ surpasses $clip(-1, r, 1)$ by 12.59% across all datasets as illustrated in Figure 6.

6 Conclusion

In this paper, BEEformer— a binarized transformer architecture with SLFN and EE for textual content has been proposed. It incorporates a differentiable piecewise approximation function for BAT to ensure that the gradient computation accounts for both the magnitude and the sign of real-valued weights. A binarized SLFN is integrated in each transformer block, for selective retention of significant information. Overall, it accomplishes a $21.30 \times$ reduction in size with minimal impact on performance compared to a full-precision model. Furthermore, it accelerates inference through an intuitive EE technique monitoring entropy changes in logits. By applying soft-routing loss during training, the losses from all exits are accounted to optimally update the weights of each transformer block. This not only reduces overall FLOPs during inference by 52.08%, but also offers a solution to the "overthinking" problem. Extensive evaluation on six benchmark datasets, showcases its ability to deliver Pareto-optimal results concerning both efficacy as well as efficiency. Additionally, the efficacy of each component in BEEformer has been validated through various ablation studies. This makes the BEEformer an apt choice for applications with a limited computational budget combined with the demand for faster inference. However, the proposed architecture has certain limitations too. The current version is based on the transformer encoder and is limited to Natural Language Understanding (NLU) tasks only. Being a dynamic architecture, it is difficult to estimate the inference time and FLOPs beforehand. Future research can focus on enhancing BEEformer with generative capabilities or even expanding its scope to multi-modal data, to boost its versatility across domains.

Acknowledgments

This study is supported by the University Grants Commission (UGC), India through a research fellowship awarded to Wazib Ansar for his Ph.D. pursuit. However, the UGC played no role in the study’s design, execution, analysis, or decision to publish the findings.

References

- [1] Q. Li et al., “A survey on text classification: From traditional to deep learning”, *ACM Transactions on Intelligent Systems and Technology (TIST)*, vol. 13, no. 2, pp. 1–41, 2022.
- [2] L. Gu, W. Zhang, Z. Wang, D. Zeng, and H. Jin, "Service management and energy scheduling toward low-carbon edge computing," *IEEE Transactions on Sustainable Computing*, vol. 8, no. 1, pp. 109–119, 2022.
- [3] S. M. Hasan, T. Islam, M. Saifuzzaman, K. R. Ahmed, C.-H. Huang, and A. R. Shahid, "Carbon emission quantification of machine learning: A review," *IEEE Transactions on Sustainable Computing*, 2025.
- [4] M. Alswaitti, R. Verdecchia, G. Danoy, P. Bouvry, and J. Pecero, "Training green AI models using elite samples," *IEEE Transactions on Sustainable Computing*, 2025.
- [5] F. Lagunas, E. Charlaix, V. Sanh, and A. M. Rush, “Block Pruning For Faster Transformers”, in *Proceedings of the 2021 Conference on Empirical Methods in Natural Language Processing*, 2021, pp. 10619–10629.
- [6] V. Sanh, “DistilBERT, a distilled version of BERT: smaller, faster, cheaper and lighter”, *arXiv preprint arXiv:1910.01108*, 2019.
- [7] S. Wang, B. Z. Li, M. Khabsa, H. Fang, and H. Ma, “Linformer: Self-attention with linear complexity”, *arXiv preprint arXiv:2006.04768*, 2020.
- [8] S. Mangrulkar, A. Ms, and V. Sembium, “Be3r: Bert based early-exit using expert routing”, in *Proceedings of the 28th ACM SIGKDD Conference on Knowledge Discovery and Data Mining*, 2022, pp. 3504–3512.
- [9] Y. Kaya, S. Hong, and T. Dumitras, “Shallow-deep networks: Understanding and mitigating network overthinking”, in *International conference on machine learning*, 2019, pp. 3301–3310.
- [10] J. Xin, R. Nogueira, Y. Yu, and J. Lin, “Early exiting BERT for efficient document ranking”, in *Proceedings of SustaiNLP: Workshop on Simple and Efficient Natural Language Processing*, 2020, pp. 83–88.
- [11] S. Shen et al., “Q-bert: Hessian based ultra low precision quantization of bert”, in *Proceedings of the AAAI Conference on Artificial Intelligence*, 2020, vol. 34, pp. 8815–8821.
- [12] Z. Yao, R. Yazdani Aminabadi, M. Zhang, X. Wu, C. Li, and Y. He, “Zeroquant: Efficient and affordable post-training quantization for large-scale transformers”, *Advances in Neural Information Processing Systems*, vol. 35, pp. 27168–27183, 2022.
- [13] Z. Liu, W. Luo, B. Wu, X. Yang, W. Liu, and K.-T. Cheng, “Bi-real net: Binarizing deep network towards real-network performance”, *International Journal of Computer Vision*, vol. 128, pp. 202–219, 2020.

- [14] M. W. U. Rahman et al., “Quantized transformer language model implementations on edge devices”, in 2023 International Conference on Machine Learning and Applications (ICMLA), 2023, pp. 709–716.
- [15] B. Rokh, A. Azarpeyvand, and A. Khanteymooori, “A comprehensive survey on model quantization for deep neural networks in image classification”, *ACM Transactions on Intelligent Systems and Technology*, vol. 14, no. 6, pp. 1–50, 2023.
- [16] H. Shen, N. Mellempudi, X. He, Q. Gao, C. Wang, and M. Wang, “Efficient post-training quantization with fp8 formats”, *Proceedings of Machine Learning and Systems*, vol. 6, pp. 483–498, 2024.
- [17] G. Shomron, F. Gabbay, S. Kurzum, and U. Weiser, “Post-training sparsity-aware quantization”, *Advances in Neural Information Processing Systems*, vol. 34, pp. 17737–17748, 2021.
- [18] M. Chen et al., “Efficientqat: Efficient quantization-aware training for large language models”, arXiv preprint arXiv:2407.11062, 2024.
- [19] H. Qin et al., “Bibench: Benchmarking and analyzing network binarization”, in *International Conference on Machine Learning*, 2023, pp. 28351–28388.
- [20] I. Hubara, M. Courbariaux, D. Soudry, R. El-Yaniv, and Y. Bengio, “Binarized neural networks”, *Advances in neural information processing systems*, vol. 29, 2016.
- [21] H. Bai et al., “BinaryBERT: Pushing the Limit of BERT Quantization”, in *Proceedings of the 59th Annual Meeting of the Association for Computational Linguistics and the 11th International Joint Conference on Natural Language Processing (Volume 1: Long Papers)*, 2021, pp. 4334–4348.
- [22] H. Qin et al., “BiBERT: Accurate Fully Binarized BERT”, in *International Conference on Learning Representations*.
- [23] Z. Liu et al., “Bit: Robustly binarized multi-distilled transformer”, *Advances in neural information processing systems*, vol. 35, pp. 14303–14316, 2022.
- [24] S. Stanton, P. Izmailov, P. Kirichenko, A. A. Alemi, and A. G. Wilson, “Does knowledge distillation really work?”, *Advances in Neural Information Processing Systems*, vol. 34, pp. 6906–6919, 2021.
- [25] Y. Han, G. Huang, S. Song, L. Yang, H. Wang, and Y. Wang, “Dynamic neural networks: A survey,” *IEEE Transactions on Pattern Analysis and Machine Intelligence*, vol. 44, no. 11, pp. 7436–7456, 2021.
- [26] B. Fu, F. Chen, P. Li, and D. Zeng, “Serving Transformer Models via Joint Request Scheduling and Batching in the Network Edge,” *IEEE Transactions on Sustainable Computing*, 2025.
- [27] J. Xin, R. Tang, J. Lee, Y. Yu, and J. Lin, “DeeBERT: Dynamic Early Exiting for Accelerating BERT Inference”, in *Proceedings of the 58th Annual Meeting of the Association for Computational Linguistics*, 2020, pp. 2246–2251.
- [28] X. Liu et al., “Towards Efficient NLP: A Standard Evaluation and A Strong Baseline”, in *Proceedings of the 2022 Conference of the North American Chapter of the Association for Computational Linguistics: Human Language Technologies*, 2022, pp. 3288–3303.
- [29] W. Ansar, S. Goswami, A. Chakrabarti, and B. Chakraborty, “A novel selective learning based transformer encoder architecture with enhanced word representation”, *Applied Intelligence*, vol. 53, no. 8, pp. 9424–9443, 2023.
- [30] W. Zhang et al., “TernaryBERT: Distillation-aware Ultra-low Bit BERT”, in *Proceedings of the 2020 Conference on Empirical Methods in Natural Language Processing (EMNLP)*, 2020, pp. 509–521.
- [31] A. Fan, E. Grave, and A. Joulin, “Reducing transformer depth on demand with structured dropout”, arXiv preprint arXiv:1909.11556, 2019.
- [32] P. Michel, O. Levy, and G. Neubig, “Are sixteen heads really better than one?”, *Advances in neural information processing systems*, vol. 32, 2019.
- [33] W. Zhou, C. Xu, T. Ge, J. McAuley, K. Xu, and F. Wei, “Bert loses patience: Fast and robust inference with early exit”, *Advances in Neural Information Processing Systems*, vol. 33, pp. 18330–18341, 2020.
- [34] A. Vaswani, “Attention is all you need”, *Advances in Neural Information Processing Systems*, 2017.
- [35] A. Conneau and D. Kiela, “Senteval: An evaluation toolkit for universal sentence representations”, arXiv preprint arXiv:1803.05449, 2018.
- [36] A. Warstadt, “Neural Network Acceptability Judgments”, arXiv preprint arXiv:1805.12471, 2019.
- [37] B. Dolan and C. Brockett, “Automatically constructing a corpus of sentential paraphrases”, in *Third international workshop on paraphrasing (IWP2005)*, 2005.
- [38] A. Wang, “Glue: A multi-task benchmark and analysis platform for natural language understanding”, arXiv preprint arXiv:1804.07461, 2018.

- [39] A. Williams, N. Nangia, and S. R. Bowman, “A broad-coverage challenge corpus for sentence understanding through inference”, arXiv preprint arXiv:1704.05426, 2017.
- [40] J. Devlin, M.-W. Chang, K. Lee, and K. Toutanova, “Bert: Pre-training of deep bidirectional transformers for language understanding”, in Proceedings of the 2019 conference of the North American chapter of the association for computational linguistics: human language technologies, volume 1 (long and short papers), 2019, pp. 4171–4186.
- [41] Z. Lan, M. Chen, S. Goodman, K. Gimpel, P. Sharma, and R. Soricut, “Albert: A lite bert for self-supervised learning of language representations”, arXiv preprint arXiv:1909.11942, 2019.
- [42] Y. Liu et al., “Roberta: A robustly optimized bert pretraining approach”, arXiv preprint arXiv:1907.11692, 2019.